Relativistic spin-polarized single-site scattering theory

1994 J. Phys.: Condens. Matter 6 3499

(http://iopscience.iop.org/0953-8984/6/19/005)

J. Phys.: Condens. Matter 6 (1994) 3499–3517. Printed in the UK

Relativistic spin-polarized single-site scattering theory

A C Jenkins and P Strange
Physics Department, University of Keele, Staffordshire ST5 5BG, UK

Received 17 January 1994, in final form 14 February 1994

Abstract. Relativistic spin-polarized scattering theory is discussed and the relevant radial Dirac equations for an electron in a potential with a magnetic field component are derived. The full solution to the coupled Dirac equations treating spin–orbit coupling and spin polarization on an equal footing is found and, by matching these wavefunctions at the muffin-tin radius, the scattering amplitudes and phase shifts are calculated. The interpretation of these results gives a pictorial view of the interplay between spin–orbit coupling and spin polarization. New coupling between states is observed due to the removal of previously used approximations. The magnitude of this coupling throws doubt on some earlier calculations of magnetocrystalline anisotropy energies. A scattering analogue to the generalized Zeeman effect is also described.

1. Introduction

It is clear that a fully satisfactory theory of the electronic structure of condensed matter must be able to give a full account of both relativistic and magnetic effects. Such a theory is required for the description of phenomena which are intrinsically relativistic such as magnetic anistropy energies (Strange *et al* 1989b) and the polarization dependence of various spectroscopies (Ebert *et al* 1991). Furthermore it is desirable to treat spin polarization and relativity on an equal footing in electronic structure. Prior to the early 1980s the usual procedure was to treat one of these as a perturbation. It is obvious, however, that there are many applications for which such an approach is not satisfactory. As an example one may cite the actinide elements where electronic properties are strongly and inseparably influenced by both effects. Also one may wish to examine the electronic structure of alloys where one component is magnetic and the other heavy and hence relativistic (e.g. $Ni_x Pt_{1-x}$). Examination of the band structure treating either magnetism or spin–orbit coupling perturbatively is clearly invalid over some parts of the concentration range.

The vast majority of present-day work on the electronic structure of condensed matter is based on the density-functional theory (Hohenberg and Kohn 1964, Kohn and Sham 1965). In the late 1970s this was generalized in order to make it applicable to systems in which a relativistic treatment of the electrons is necessary (Macdonald and Vosko 1979, Rajagopal 1978, Ramana and Rajagopal 1979). In particular MacDonald and Vosko developed the theory for a many-electron system in the presence of a 'spin-only' magnetic field. Although this theory ignores diamagnetic effects it is still a suitable basis for treating the problem we have referred to above.

In the mid 1980s this problem was tackled by Strange *et al* (1984) and also by Feder *et al* (1983). In particular Strange *et al* demonstrated how to solve the problem of an electron scattering from a single effective potential with a magnetic component. The scattering parameters from this were used in a multiple scattering theory (Strange *et al* 1989a) to perform relativistic KKR calculations (Korringa 1947, Kohn and Rostoker 1954). From

0953-8984/94/193499+19$19.50

this work many observables have been calculated such as magnetic anisotropy energies (Strange *et al* 1989c), hyperfine fields (Ebert *et al* 1988), magnetic dichroism (Ebert *et al* 1991, Strange *et al* 1991) and magneto-x-ray effects (Strange and Gyorffy 1990, Gotsis and Strange 1994).

As was shown by Strange *et al* (1984) the radial Kohn–Sham–Dirac equation for an electron experiencing a potential with a magnetic component becomes two infinite sets of coupled partial differential equations, one set for even and the other set for odd values of the l quantum number, for each value of the m_j quantum number. By neglecting coupling between states l and $l \pm 2$ they were able to reduce this to sets of four coupled partial differential equations, find the solutions, and incorporate them into a single-site scattering theory. In this paper we reintroduce this coupling to give a complete solution of the Dirac equation in the presence of a spin-only magnetic field.

Ackermann and Feder (1984) have briefly discussed the solution of the radial equations including the full coupling. However, they give little discussion of the details of how they treated the infinite set of coupled equations, and simply state that the effect is negligible for their purposes. Here, we present a careful and detailed study of the effect of the extra coupling on the single-site scattering, and show that it may well be of significance in the calculation of certain quantities in condensed-matter physics.

In the next section we mention the relativistic density functional theory. Then we go on to write down and solve the radial Dirac equations for this case. Next we develop a fully relativistic single site scattering theory and use our solutions of the Dirac equation to calculate $\mathbf{t}$ matrices and scattering amplitudes. As an example we apply this theory to scattering from a single magnetic platinum atom, explicitly calculating resonance energies, leading to the Zeeman effect. Finally, we discuss the extension of this work to multiple-scattering theory, and its implications for the calculations of observables.

2. Theory

Density functional theory can be used to study the properties of relativistic electron systems in the presence of external fields. It has been shown (Rajagopal 1978, Macdonald and Vosko 1979) that the ground state energy of such a system with external fields $(V^{\mathrm{ext}}, A^{\mathrm{ext}})$ is indeed a functional of the ground state four-current $(n(r), J(r))$. If the Gordon decomposition of the current (Baym 1974) is applied and diamagnetic effects ignored then the Kohn–Sham–Dirac equations reduce to

$$(-i\hbar c\alpha \cdot \nabla + \beta mc^2 + V^{\mathrm{eff}}[n, m] + \beta\sigma \cdot B^{\mathrm{eff}}[n, m] - \epsilon_i)\varphi_i(r) = 0 \tag{1}$$

where

$$m(r) = \sum_i^{\mathrm{occ}} \mathrm{Tr}\varphi_i^\dagger(r)\beta\sigma\varphi_i(r) \tag{2}$$

$$V^{\mathrm{eff}}(r) = -\left(V^{\mathrm{ext}}(r) + \frac{\delta E_{\mathrm{xc}}^{\mathrm{r}}}{\delta n(r)} + e^2\int \frac{n(r')}{|r - r'|}\mathrm{d}r'\right) \tag{3}$$

$$B^{\mathrm{eff}}(r) = \frac{e\hbar}{2mc}\left(B^{\mathrm{ext}}(r) + \frac{\delta E_{\mathrm{xc}}^{\mathrm{r}}[n, m]}{\delta m(r)}\right). \tag{4}$$

$E_{\mathrm{xc}}^{\mathrm{r}}$ is the relativistic exchange–correlation energy functional. $B^{\mathrm{ext}}(r)$ is a fictitious magnetic field which couples to the 'spin-only' current and σ, β and α are the usual relativistic

matrices in the standard representation. In the non-relativistic limit these equations reduce to the Kohn–Sham-Pauli equations (Von Barth and Hedin 1972). This formalism isolates the dominant part of the problem of the magnetism in metals and alloys in which relativistic effects are also important.

The first requirement in the development of a first-principles band-structure method based on the density-functional theory is a solution of the above equations for the case where the potential and field are those associated with a single scattering centre (Lloyd and Smith 1972). $B^{\text{eff}}(r)$ is taken to be along the z-axis and both $V^{\text{eff}}(r)$ and $B^{\text{eff}}(r)$ are assumed to be spherically symmetric inside the muffin-tin radius and constant, often chosen to be zero, outside i.e.

$$V^{\text{eff}}(r) = \begin{cases} V^{\text{eff}}(r) & \text{if } r < r_{\text{m}} \\ \text{constant} & \text{if } r > r_{\text{m}} \end{cases} \tag{5}$$

and

$$B^{\text{eff}}(r) = \begin{cases} B^{\text{eff}}(r) & \text{if } r < r_{\text{m}} \\ \text{constant} & \text{if } r > r_{\text{m}} \end{cases} \tag{6}$$

Using the Lippmann–Schwinger equation (Newton 1966) it has been shown (Strange *et al* 1984, Feder *et al* 1983) that the Kohn–Sham–Dirac equation can be separated into angular and radial parts for this potential and field. The radial part is

$$\frac{\partial(rcf^{m_j}_{\kappa'\kappa}(r))}{\partial r} = \kappa c f^{m_j}_{\kappa'\kappa}(r) - (E - V^{\text{eff}}(r)) r g^{m_j}_{\kappa'\kappa}(r) + B^{\text{eff}}(r) \sum_{\kappa''} G(\kappa'', \kappa', m_j) r g^{m_j}_{\kappa''\kappa}(r) \tag{7}$$

$$\frac{\partial(rg^{m_j}_{\kappa'\kappa}(r))}{\partial r} = -\kappa g^{m_j}_{\kappa'\kappa}(r) + \left(\frac{E - V^{\text{eff}}(r)}{c^2} + 1\right) r c f^{m_j}_{\kappa'\kappa}(r) + B^{\text{eff}}(r) \sum_{\kappa''} G(-\kappa'', -\kappa', m_j) c r f^{m_j}_{\kappa''\kappa}(r) \tag{8}$$

where κ is the usual spin-angular quantum number and

$$G(\kappa, \kappa', m_j) = \text{Tr} \int \mathrm{d}r\, \chi^{m'_j}_{\kappa'}(\hat{r}) \sigma_z \chi^{m_j}_{\kappa}(\hat{r}) \tag{9}$$

The first index κ' indicates the component of Ψ belonging to that specific value of κ', i.e. the component from which the relative probability of finding the particles with these values of total and orbital angular momenta can be found. The second, κ, is used to define the corresponding properties of the incident beam and thus provide a boundary condition. m_j is conserved in the scattering process. The extra coupling due to the magnetic field is apparent and is determined by non-zero values of $G(\kappa, \kappa', m_j)$ which occur between $j = l + \frac{1}{2}$ and $j = l - \frac{1}{2}$ ($\kappa = -l - 1$ and $\kappa = l$ respectively) and also between l and $l \pm 2$. The coupling between $l \pm 2$ has been ignored in previous work as it is small if the field or field gradient is small. The following work will include, rather than neglect, this $l \pm 2$ coupling.

If the coupling between $l \pm 2$ channels is included then the equations return to being a set of infinite coupled equations! These equations separate into two sets, one for odd l and another set for even l, due to parity of the wavefunction. In order to solve these coupled equations an approximation has to be implemented. Strange *et al* (1984) neglected coupling between l and $l \pm 2$ as it is of the order of $1/c^4$. Coupling between l and $l \pm 4$ is very small especially for low energies, and this is our chosen cut-off point i.e. for dominant $l = 2$ we discount contributions from $l = 6, 8, 10$, etc. Obviously $l = 2$ is coupled to both $l = 0$ and $l = 4$ so we have to include the coupling between $l = 0$ and $l = 4$, even though it is small, to make the equations self-consistent.

2.1. Numerical methods

The coefficients of $G(\kappa, \kappa', m_j)$ are given in terms of Clebsch–Gordan coefficients, and in the notation of Rose (1961), as

$$G(\kappa, \kappa', m_j) = C\left(l\frac{1}{2}j; m_j - \frac{1}{2}\frac{1}{2}\right)C\left(l'\frac{1}{2}j; m_j - \frac{1}{2}\frac{1}{2}\right) - C\left(l\frac{1}{2}j; m_j + \frac{1}{2} - \frac{1}{2}\right)C\left(l'\frac{1}{2}j; m_j + \frac{1}{2} - \frac{1}{2}\right) \tag{10}$$

and, as already mentioned, the radial Dirac equations are an infinite set of coupled non-linear partial differential equations. Since we are going to neglect coupling to values of $l \geqslant 6$, the equations will separate into a finite set of linear simultaneous partial differential equations which makes the solution tractable. These equations can be solved using an adaptation of the method described by Loucks (1967) and Strange *et al* (1984). This involves using the Milne method with the wavefunction at the first six grid points calculated using the Runga–Kutta method. Loucks' method is for two coupled equations and Strange *et al* extended this to four. This method can easily be generalized to n coupled equations where n is dependent on m_j and $2 \leqslant n \leqslant 12$.

Initializing the integration is a straightforward generalization of the method of Loucks (1967). A series solution near to the origin is taken. It takes the form

$$\begin{Bmatrix} \cdots \\ \cdots \\ \mathrm{i}f_{\kappa\kappa'}^{m_j} \\ g_{\kappa\kappa''}^{m_j} \\ \mathrm{i}f_{\kappa\kappa''}^{m_j} \\ g_{\kappa\kappa'''}^{m_j} \\ \cdots \\ \cdots \end{Bmatrix} \underset{\longrightarrow}{r \to 0} \begin{Bmatrix} \cdots \\ \cdots \\ 0 \\ 1 \\ \rho(\kappa_i) \\ 0 \\ \cdots \\ \cdots \end{Bmatrix} r^{s(\kappa_i)} \tag{11}$$

and, as the ratios of $f_{\kappa\kappa'}/g_{\kappa\kappa'}$ for all applicable couplings are all that are required, normalization is not necessary.

If these wavefunctions are examined in the limit $c \to \infty$ then the results are consistent with those found from a Pauli-like equation in the spin-up–spin-down representation. A further check on the validity of the results obtained for the wavefunctions evaluated at r_m is to take $B \to \infty$ and in this limit the results are the same as those obtained from standard integral routines i.e. when there is no coupling due to the absence of a magnetic field.

3. Matching the wavefunctions at the muffin-tin radius

If it is assumed that both the potential, $V^{\text{eff}}(r)$, and the magnetic field, $B^{\text{eff}}(r)$, are zero outside the muffin-tin radius, r_m, then the radial solutions outside the muffin-tin sphere have the form

$$\Psi_{\text{outside}}(r) = \begin{Bmatrix} j_{l_1}(pr)\delta_{\kappa_1,\kappa} - \mathrm{i}ph_{l_1}^{+}(pr)t_{\kappa_1,\kappa}^{m_j}(\epsilon) \\ [\mathrm{i}p/p_0 + 1]S_{\kappa_1}(j_{\bar{l}_1}(pr)\delta_{\kappa_1,\kappa} - \mathrm{i}ph_{\bar{l}_1}^{+}(pr)t_{\kappa_1,\kappa}^{m_j}(\epsilon)) \\ \cdots \\ \cdots \\ j_{l_n}(pr)\delta_{\kappa_n,\kappa} - \mathrm{i}ph_{l_n}^{+}(pr)t_{\kappa_n,\kappa}^{m_j}(\epsilon) \\ [\mathrm{i}p/p_0 + 1]S_{\kappa_n}(j_{\bar{l}_n}(pr)\delta_{\kappa_n,\kappa} - \mathrm{i}ph_{\bar{l}_n}^{+}(pr)t_{\kappa_n,\kappa}^{m_j}(\epsilon)) \end{Bmatrix} \tag{12}$$

for which the index κ denotes the values of the orbital and total angular momenta of the component of the incident beam which is the boundary condition of the system. The two solutions, Ψ_{outside} and Ψ_{inside}, are matched at the muffin-tin radius and from this system of linear equations the **t** matrices can be evaluated.

$$\Psi_{\text{inside}}(r) = \sum_{\kappa} a_{\kappa} \begin{Bmatrix} g^{m_j}_{\kappa_1,\kappa}(r) \\ \mathrm{i} f^{m_j}_{\kappa_1,\kappa}(r) \\ \cdots \\ \cdots \\ g^{m_j}_{\kappa_n,\kappa}(r) \\ \mathrm{i} f^{m_j}_{\kappa_n,\kappa}(r) \end{Bmatrix}. \tag{13}$$

In principle this is the matching of two infinite column vectors for each value of κ $(= \kappa_1, ..., \kappa_n, ...)$—but, due to the cut-off in l and the fact that m_j remains a good quantum number, this reduces to, at worst, the matching of two 12 component vectors. These vectors are in the form of 12 linear simultaneous equations which, with a little algebraic manipulation, can be rearranged to form a matrix equation of the form

$$\mathbf{A}X = \mathbf{B} \tag{14}$$

with a_{κ} forming half of the column vector X and $t^{m_j}_{\kappa\kappa'}$ forming the other half. This system can be solved, for each κ, using standard routines and so we obtain, numerically, the **t**-matrix components for all couplings as a function of energy. These **t**-matrix components must satisfy the optical theorem which mixes all the components of the **t** matrix

$$t^{m_j}_{\kappa,\kappa'}(\epsilon) - t^{m_j\dagger}_{\kappa',\kappa}(\epsilon) = -2\mathrm{i}p \sum_{\kappa_1} t^{m_j}_{\kappa,\kappa_1}(\epsilon) t^{m_j\dagger}_{\kappa',\kappa_1}(\epsilon). \tag{15}$$

This ensures the conservation of particles during the scattering process. Obviously

$$t^{m_j}_{\kappa,\kappa'} = t^{m_j}_{\kappa',\kappa} \tag{16}$$

as the coupling is symmetrical.

The partial wave scattering amplitude is defined as

$$f^{m_j}_{\kappa\kappa'}(\epsilon) = -\epsilon^{1/2} t^{m_j}_{\kappa\kappa'}(\epsilon). \tag{17}$$

When $f_{\kappa\kappa'}(\epsilon)$ has no off-diagonal elements a consequence of the optical theorem is that $f_{\kappa\kappa'}$ lies on the unitary circle of the Argand plot with its centre $(0, 0.5)$. The scattering is absorptive if $f_{\kappa\kappa'}$ is within the circle and emissive if it is outside. Thus the diagonal scattering amplitude can be written

$$f_{\kappa\kappa}(\epsilon) = \frac{1}{2\mathrm{i}}(\mathrm{e}^{2\mathrm{i}\delta_{\kappa\kappa}(\epsilon)} - 1) \tag{18}$$

which defines the phase shifts $\delta_{\kappa\kappa}(\epsilon)$. These phase shifts, corresponding to the muffin-tin potential, have a resonance i.e. a characteristic s-shaped rise in $\delta(\epsilon)$ as a function of energy. The point where $\delta(\epsilon) = \pi/2$ is referred to as the resonance energy (ϵ_{r}). If the resonance energy is plotted as a function of B^{ext} a diagram analogous to that for the Zeeman splitting is obtained.

In our case we do not have diagonal scattering amplitudes, so the above theory cannot be applied directly to find the phase shifts and hence the resonance energies. However, our scattering amplitudes can be put into diagonal form by use of a similarity transform:

$$\mathbf{F}_Q(\epsilon) = U_Q^{\dagger}\mathbf{F}_\kappa(\epsilon)U_Q \tag{19}$$

where $\mathbf{F}_\kappa$ is the matrix of scattering amplitudes in the (κ, m_j) representation and $\mathbf{F}_Q$ is the matrix of scattering amplitudes in its diagonal representation. Unfortunately, in the diagonal representation we do not know the good quantum numbers (except for m_j); however we can still define a phase shift in analogy with the equation above.

4. Example of Pt

4.1. The magnetic field

In order to obtain a physically clear and useful understanding of the above formal solutions, it is appropriate to consider a simple illustrative example in which the relative sizes of the spin–orbit coupling and spin-polarization effects can vary through a large range. For this purpose it is viable to consider a muffin-tin potential well that corresponds to a single atom in a platinum crystal in the presence of an applied external magnetic field B^{ext}. The total effective magnetic field B^{eff} has therefore contributions from the induced magnetic moments due to B^{ext}.

B^{ext} induces a moment

$$m(r) = B^{\text{ext}} \int \chi_{\text{susc}}(r, r')\, \mathrm{d}r' \tag{20}$$

where χ_{susc} is the paramagnetic susceptibility of platinum. This leads to

$$\int_{\text{site}} m(r)\, \mathrm{d}r = m = B^{\text{ext}}\chi_{\text{susc}} = \frac{B^{\text{ext}}\chi_0}{1 - In(\epsilon_{\text{F}})} \tag{21}$$

by integrating over the spherically symmetric Wigner–Seitz sphere. Here χ_0 is the non-interacting susceptibility, I is the Stoner parameter and $n(\epsilon_{\text{F}})$ the relativistic density of states at the Fermi energy obtained from MacDonald *et al* (1981). Now if we assume that

$$m(r) = m\gamma_0\left(\int_{\text{site}} \gamma_0(r)\mathrm{d}r\right)^{-1} = mf(r) \tag{22}$$

in which $\gamma_0(r)$ is the spherical component of the magnetic form factor also given by MacDonald *et al* (1981), it follows that the effective magnetic field is

$$B^{\text{eff}}(r) = B^{\text{ext}} - \int \mathrm{d}r' G_{\text{xc}}[r, r', n]m(r') = B^{\text{ext}} - J(n(r))m(r) \tag{23}$$

where

$$G_{\text{xc}} = \frac{\delta^2 E_{\text{xc}}^{\text{r}}}{\delta m(r)\delta m(r')} \tag{24}$$

and

$$J(n(r)) = n(r)\frac{\delta^2 \epsilon_{\text{xc}}}{\delta m(r)^2}|_{m=0} \tag{25}$$

in the local spin density functional approximation. Finally

$$B^{\text{eff}}(r) = B^{\text{ext}}\left[1 - \frac{J(n(r))\chi_0 f(r)}{1 - In(\epsilon_{\text{F}})}\right] \tag{26}$$

Throughout our results we will work in dimensionless units (du) where 1 du = $(0.06e\hbar/2mc)B^{\text{ext}}$.

5. Results

A very common feature of the $l = 2$ phase shifts corresponding to the muffin-tin potential in transition metals is a resonance, a characteristic sharp rise in $\delta_2(E)$ as a function of energy. The point where $\delta_2(E) = \pi/2$ corresponds to the point where the scattering amplitude is purely real. The energy at which this occurs is known as the resonance energy. With no external field the scattering amplitude in the (κ, m_j) representation is diagonal and corresponds to resonant scattering in the $j = \frac{3}{2}$ and $j = \frac{5}{2}$ channels. In figure 1 we show the phase shifts as a function of energy for this case.

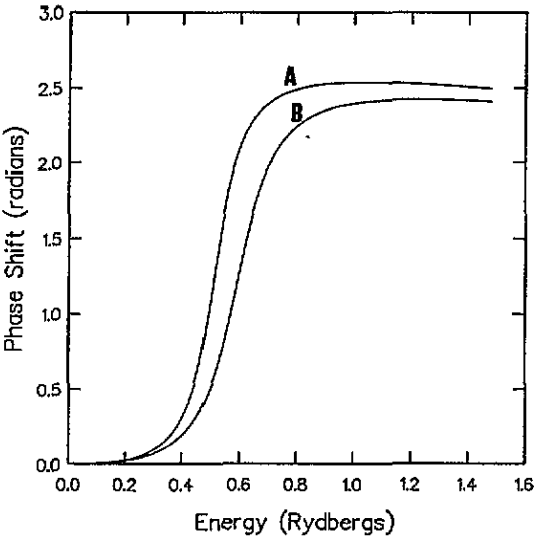

Figure 1. The platinum $j = \frac{3}{2}$ ($\kappa = 2$) (A) and $j = \frac{5}{2}$ ($\kappa = -3$) (B) phase shifts for $l = 2$.

Figures 2–4 show Argand plots of the scattering amplitudes as a function of magnetic field in the (κ, m_j) representation. The field increases linearly. In figures 2 and 3 the zero-field case is the unitarity circle and the field increases as one goes inwards. In figure 4 the zero-field case is zero at all energies, and as the field increases the scattering amplitude becomes increasingly non-circular. These figures are shown for two reasons: firstly because they are a standard way of displaying scattering amplitudes and secondly to facilitate direct comparison with the earlier work of Strange *et al* (1984). However such figures do not tell the whole story as the energy dependence of the resonance is hidden in these figures. Therefore in figures 5–7 we redisplay these results as three-dimensional plots which enables us to display qualititively the energy dependence of the scattering amplitudes. In figures 5 and 6 the resonance in the phase shift is represented as a complete twist of the scattering amplitude. For the largest fields used here the off-diagonal scattering represented by figure 7 is of the same order as the diagonal scattering.

We can see from these figures that, as the field increases, the diagonal scattering amplitudes leave the unitarity circle, and at the same time the off-diagonal components between (κ, m_j) and $(-\kappa - 1, m_j)$ appear. This must occur if we are to satisfy the optical theorem. Eventually a second loop appears in the diagonal elements of the scattering amplitude. This corresponds to the appearance of two peaks in the scattering cross section,

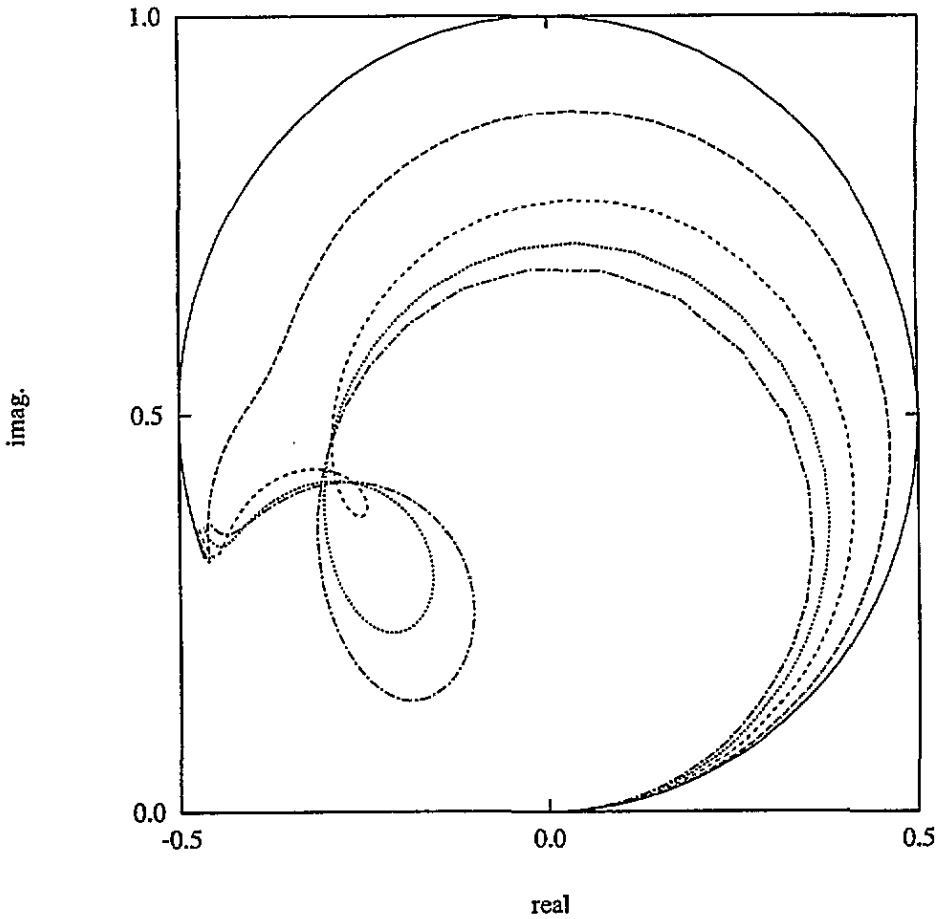

Figure 2. The $\kappa = 2$, $m_j = \frac{1}{2}$ component of the scattering amplitude as a function of magnetic field. Field increases linearly.

and comparison with figure 7 shows that it corresponds with the appearance of a kink in the off-diagonal scattering amplitude. In the scattering cross section this would appear as the emergence of two peaks so that the state with quantum numbers (κ, m_j) is now scattering significantly to states with quantum numbers $(-\kappa - 1, m_j)$ as well as (κ, m_j). As the field continues to increase the loops become larger and the kink in figure 7 more pronounced. This corresponds to an increasing separation of the peaks as might be expected.

Figures 8 and 9 show the most important of the new couplings. This is the coupling of $j = \frac{1}{2}, l = 0$ to $j = \frac{3}{2}, l = 2$ and $j = \frac{5}{2}, l = 2$. In this and all subsequent three-dimensional Argand plots the zero-field case is represented by a vertical line through the origin and parallel to the energy axis. Increasing field is represented by the graphs moving further away from this case. Clearly, these off-diagonal scattering amplitudes have significant structure and it can be seen that they are small, but appreciable, at the resonance energy.

Figures 10–13 show the coupling between $l = 2$ and $l = 4$. Evidently this is smaller still. Clearly the coupling to $\kappa = 4$ is notably larger than the coupling to $\kappa = -5$ although they both correspond to $l = 4$. This is because the wavefunctions $g^{m_j}_{4,2}$ and $f^{m_j}_{4,2}$ occur in a differential equation for $g^{m_j}_{-3,2}$ and $f^{m_j}_{-3,2}$ whereas $g^{m_j}_{-5,2}$ and $f^{m_j}_{-5,2}$ do not, and similarly for

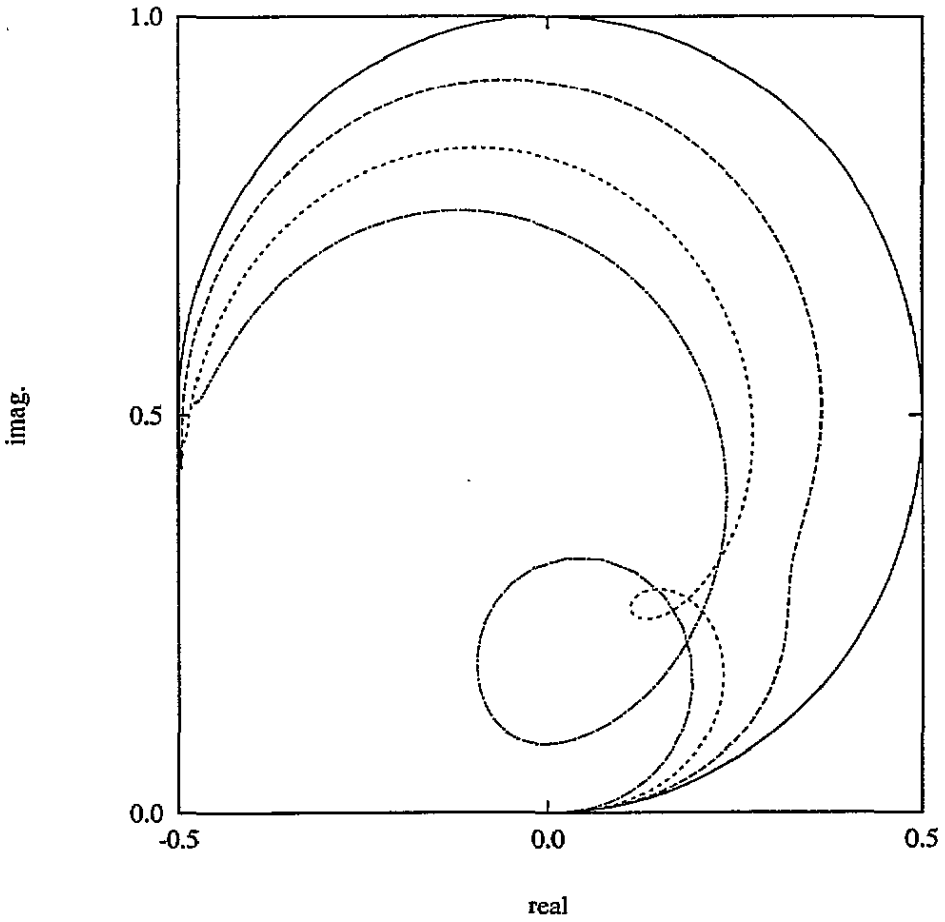

Figure 3. The $\kappa = -3$, $m_j = \frac{1}{2}$ component of the scattering amplitude as a function of magnetic field. Field increases linearly.

$\kappa' = -3$. Hence the coupling of $l = 2$ states to $\kappa = -5$ is of the order of $1/c^2$ of the coupling to $\kappa = 4$.

Figures 14 and 15 show the coupling between $l = 0$ and $l = 4$. As expected this coupling is very small but its inclusion is necessary for the **t**-matrix components to satisfy the optical theorem accurately.

We have also calculated the scattering amplitudes for the odd values of the l quantum number. However metallic platinum has only a very small amount of odd l character around the Fermi energy and so the odd scattering amplitudes are not very structured and so we do not display them explicitly. We can also, of course, calculate the scattering amplitudes for $\kappa = \kappa' = 4$ or -1 for example, and it was necessary to do this when we solved the equations above. However, such calculations can be done using standard programs and are not new, so we do not display those scattering amplitudes here.

The **t** matrices can be written in a more familiar lms representation using

$$t_{l,m_j-m_s,m_s,l',m_j-m'_s,m'_s} = \sum_{\kappa\kappa'} C(l\tfrac{1}{2}j; m_j - m_s m_s) t^{m_j}_{\kappa\kappa'} C(l'\tfrac{1}{2}j'; m'_j - m'_s m'_s). \tag{27}$$

For $l = l'$ the **t** matrices in the l, m, s representation are shown by Strange *et al* (1984). For

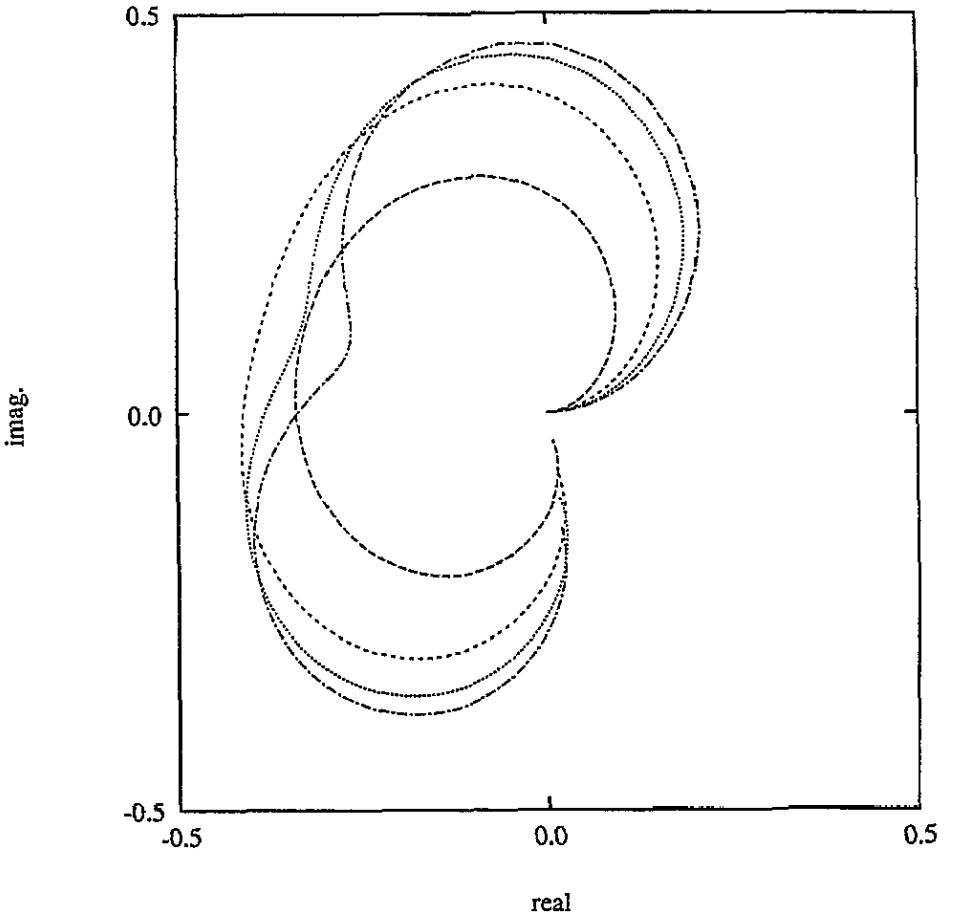

Figure 4. The $\kappa = -3$, $\kappa' = 2$, $m_j = \frac{1}{2}$ component of the scattering amplitude as a function of magnetic field. Field increases linearly from zero.

$l \neq l'$ the coupling is very small and writing the scattering amplitudes in this representation does not give any further insight into the scattering process.

We have diagonalized the scattering amplitude matrix using the prescription described above and defined phase shifts. These are shown in figure 16 for the $l = 2$ levels of platinum and for a magnetic field of one dimensionless unit. The lower (in energy) four phase shifts are the ones that have $j = \frac{3}{2}$ in the non-magnetic limit; the higher six phase shifts correspond to the $j = \frac{5}{2}$ case in the non-magnetic limit. Compare this figure with figure 1. Finding the phase shifts for many fields has enabled us to examine the Zeeman effect and the result of this is shown in figure 17. This is similar to the results of Strange *et al* (1984). At the low-field end of this figure we have the Zeeman effect of two spin–orbit split levels slightly split by the magnetic field. At the high-field end we have five spin-up and five spin-down levels slightly split by the spin–orbit coupling. The intermediate region between these cases is around one dimensionless unit where we can see one level has left the $j = \frac{5}{2}$ levels and is heading for the lower group of levels. This can also be seen in the phase shifts of figure 16 where one phase shift is in the middle of the two main groups of phase shifts. There is one noteworthy difference from the earlier work in the present results. At the high field end the levels are equally spaced here, but in the previous work

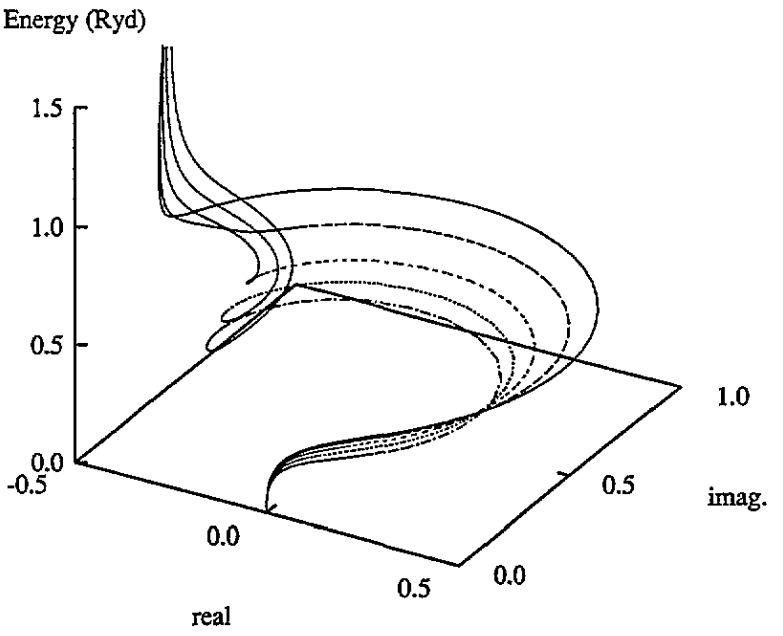

Figure 5. The $\kappa = 2$, $m_j = \frac{1}{2}$ component of the scattering amplitude as a function of energy for the same magnetic fields as in figure 2.

there was a notably larger splitting between the more negative m_j levels than between the higher m_j levels.

6. Discussion

The single-site scattering theory presented here is a direct generalization of the work of Strange *et al* (1984). In the correct limit it reduces to their theory. Furthermore, in the limit $c \rightarrow \infty$ it reduces to the non-relativistic scattering theory described by Gyorffy (1982) for example. As the magnetic field $B \rightarrow 0$ this work reduces to the relativistic single-site scattering theory discussed by Staunton and co-workers (1980) for example. All these authors have discussed the generalization of their work to multiple scattering. This is facilitated by the fact that the multiple scattering problem can be separated into a part which depends only on the single-site scattering **t** matrices and a part which depends only on the geometry of the scattering centres. Furthermore, the formal theory of multiple scattering does not depend upon the details of the quantum number coupling of the **t** matrices, so Strange *et al* (1989a) were able to derive a multiple scattering theory for the relativistic spin-polarized case (when the $l, l\pm2$ coupling is ignored) by analogy with the non-relativistic theory . Clearly much of the work discussed in their paper can be carried over when the theory presented here is generalized to multiple scattering.

This paper represents a first important step in the development of a new multiple-scattering formalism. Such a multiple scattering theory can be used in a KKR framework to calculate the electronic structure of magnetic materials. Development of such a theory is under way. There is only good reason to do this if such a theory can give us new insight

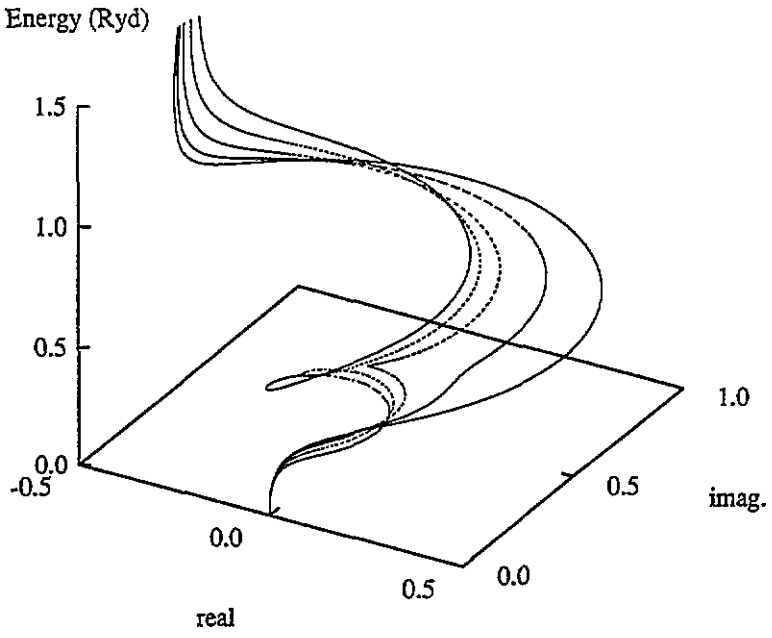

Figure 6. The $\kappa = -3$, $m_j = \frac{1}{2}$ component of the scattering amplitude as a function of energy for the same magnetic fields as in figure 3.

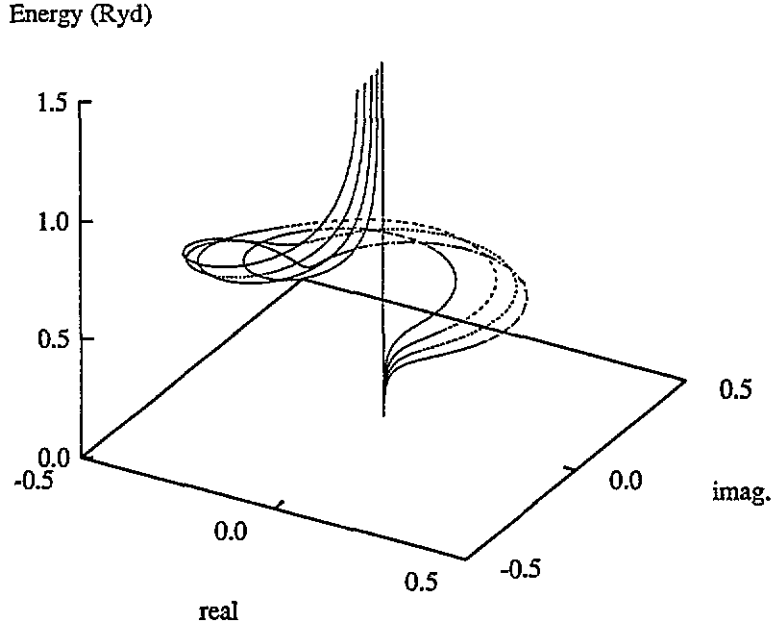

Figure 7. The $\kappa = -3$, $\kappa' = 2$, $m_j = \frac{1}{2}$ component of the scattering amplitude as a function of energy for the same magnetic fields as in figure 4.

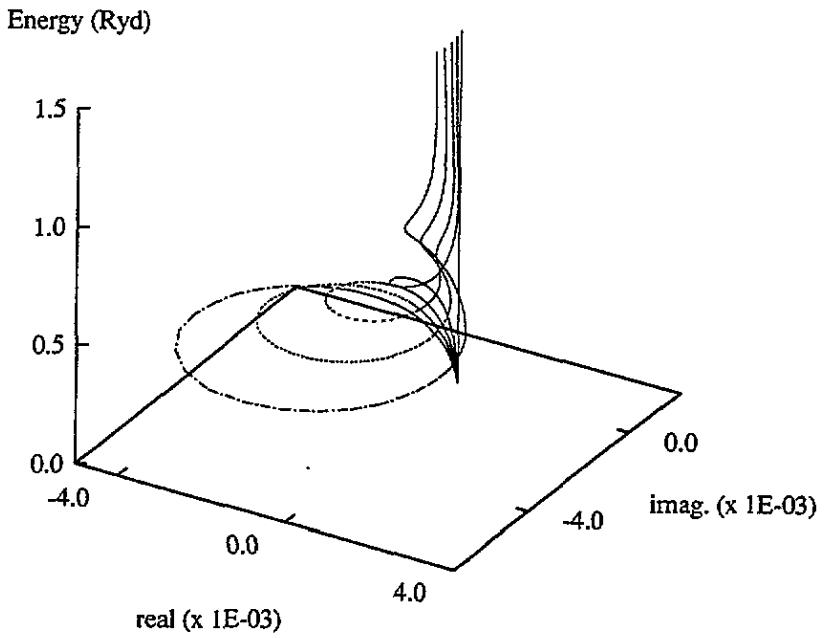

Figure 8. The $\kappa = -1$, $\kappa' = 2$, $m_j = \frac{1}{2}$ component of the scattering amplitude as a function of energy for the same magnetic fields as in figure 4.

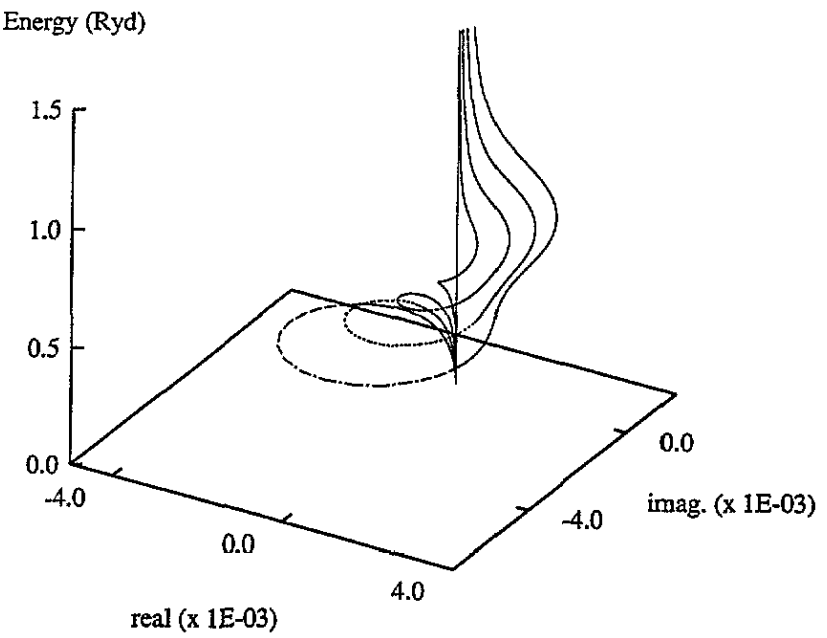

Figure 9. The $\kappa = -1$, $\kappa' = -3$, $m_j = \frac{1}{2}$ component of the scattering amplitude as a function of energy for the same magnetic fields as in figure 4.

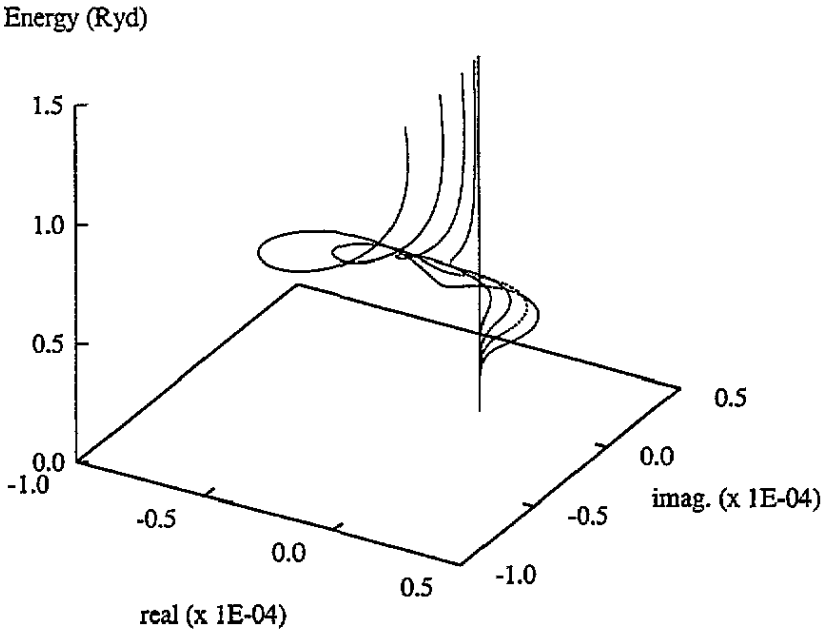

Figure 10. The $\kappa = 2$, $\kappa' = 4$, $m_j = \frac{1}{2}$ component of the scattering amplitude as a function of energy for the same magnetic fields as in figure 4.

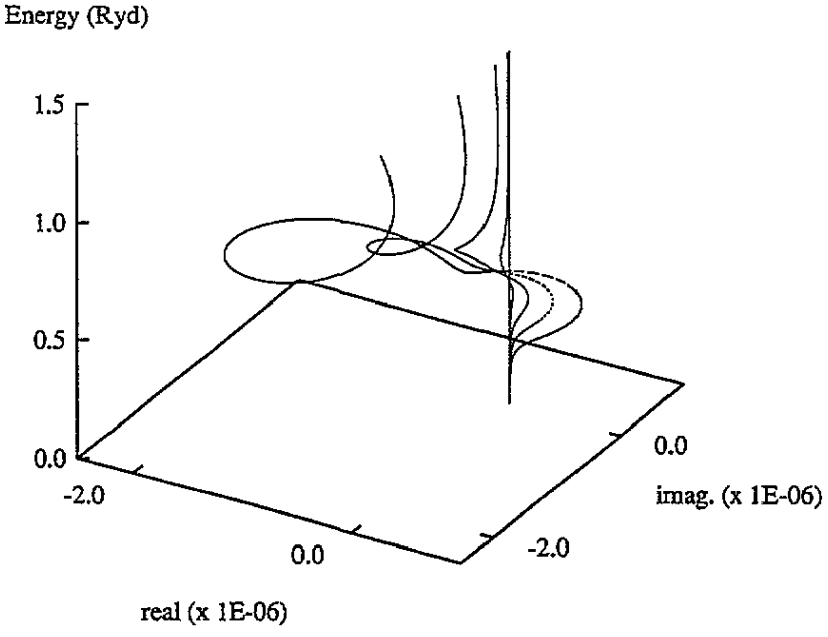

Figure 11. The $\kappa = 2$, $\kappa' = -5$, $m_j = \frac{1}{2}$ component of the scattering amplitude as a function of energy for the same magnetic fields as in figure 4.

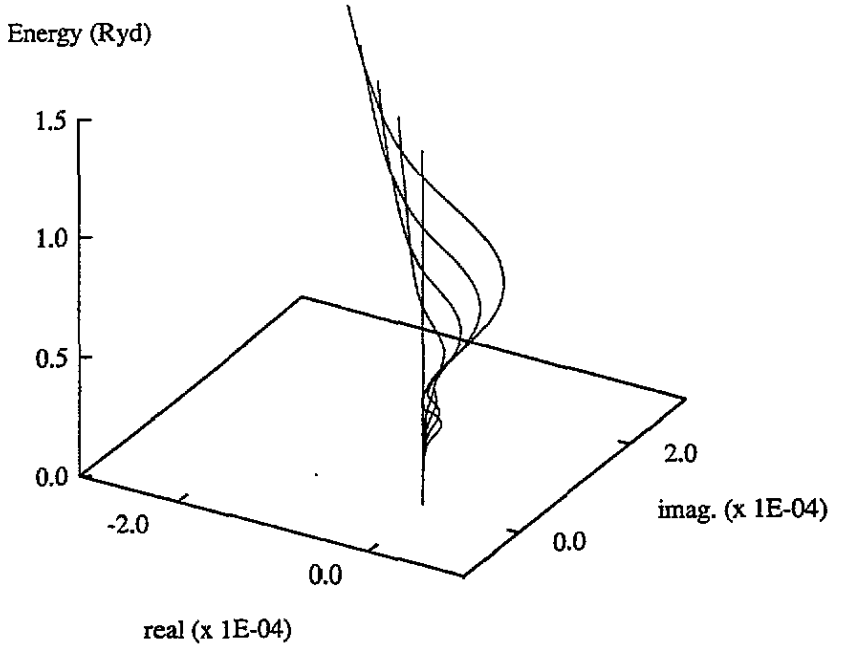

Figure 12. The $\kappa = -3$, $\kappa' = 4$, $m_j = \frac{1}{2}$ component of the scattering amplitude as a function of energy for the same magnetic fields as in figure 4.

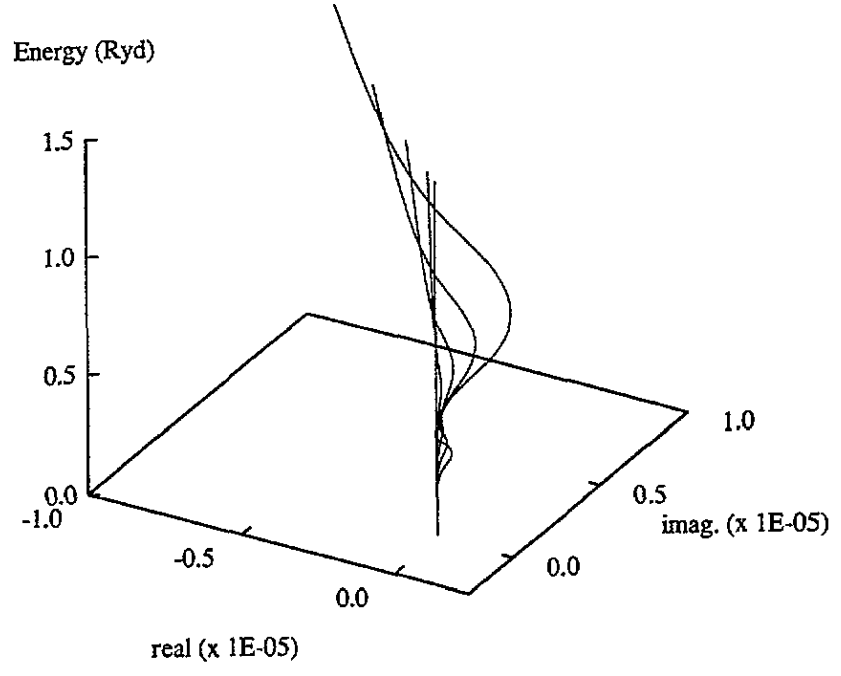

Figure 13. The $\kappa = -3$, $\kappa' = -5$, $m_j = \frac{1}{2}$ component of the scattering amplitude as a function of energy for the same magnetic fields as in figure 4.

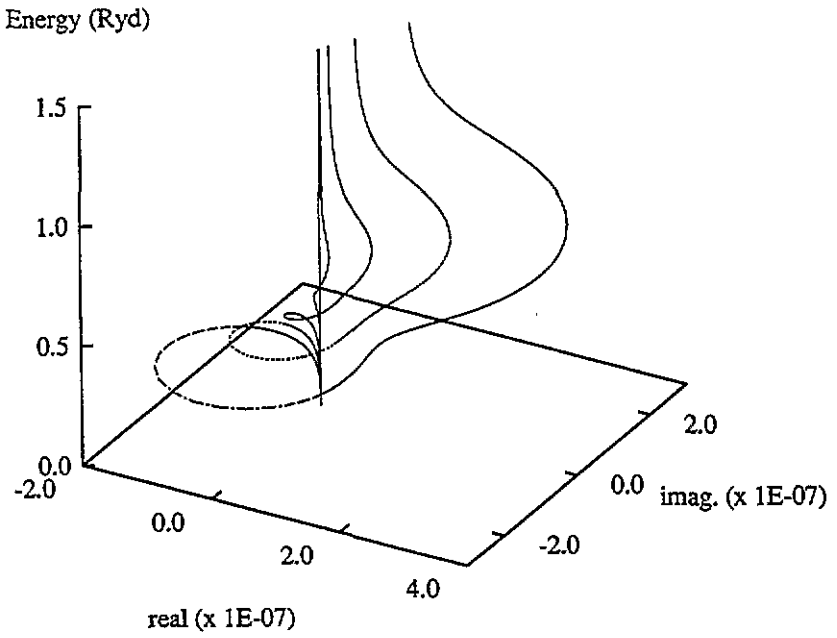

Figure 14. The $\kappa = -1$, $\kappa' = 4$, $m_j = \frac{1}{2}$ component of the scattering amplitude as a function of energy for the same magnetic fields as in figure 4.

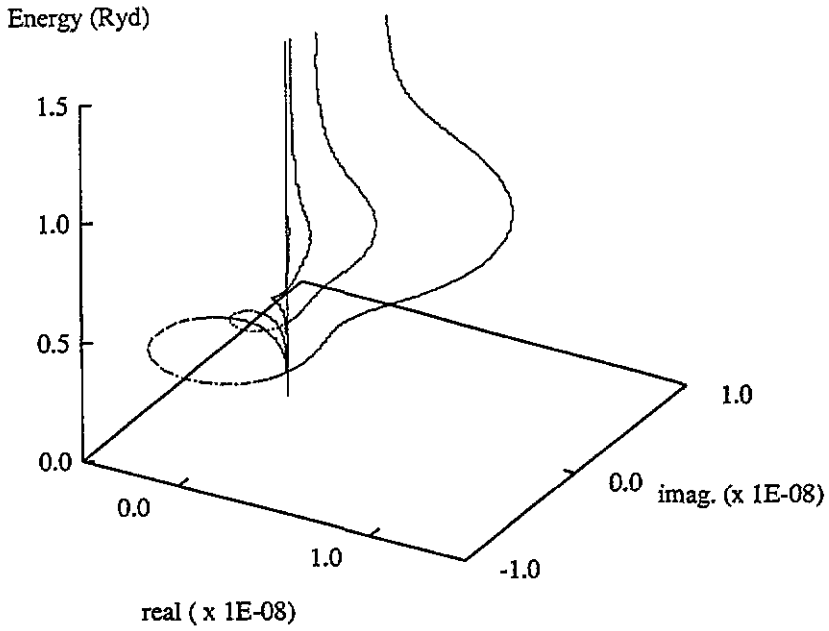

Figure 15. The $\kappa = -1$, $\kappa' = -5$, $m_j = \frac{1}{2}$ component of the scattering amplitude as a function of energy for the same magnetic fields as in figure 4.

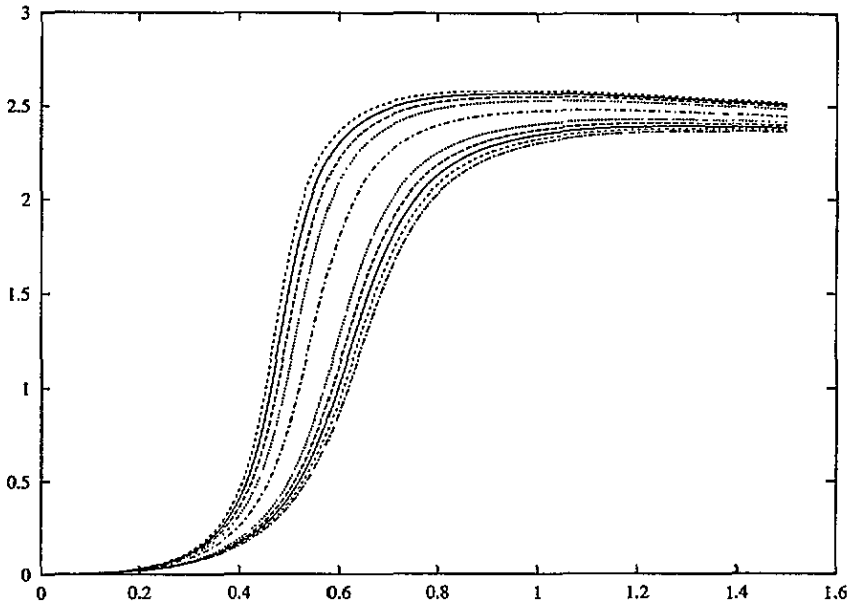

Figure 16. The phase shifts as a function of energy for the $l = 2$ levels in Pt. The central dot-dash line is $m_j = -2.5$, the dotted lines are $m_j = -1.5$ and the full lines $m_j = 0.5$. As m_j changes by one unit from one phase shift to the next, the values of m_j for all other phase shifts can be determined.

into the properties of materials, and can calculate quantities not calculable within a less sophisticated theory. Two examples of such quantities are as follows.

Firstly, several authors have attempted to use the theory of Strange *et al* (1989a) or theories equivalent to it to calculate magnetocrystalline anisotropy energies in transition metals from first principles, and have met with varying degrees of success (see Strange *et al* (1989b, 1991), Daalderop *et al* (1989), Guo *et al* (1992) for example). First-principles calculation of these energies is fraught with technical difficulties as they are of the order of microelectronvolts. Even if these problems can be overcome reliably the theory presented here shows that if this new coupling is not included such calculations may well yield incorrect answers. Figures 8 and 9 show that the previously ignored $l, l \pm 2$ coupling affects the **t** matrices in the third/fourth significant figure. It is not clear what effect a change in the third/fourth figure of the scattering amplitude at a particular energy will have on an energy integrated quantity like magnetocrystalline anisotropy energy. However, the scattering amplitude appears in the KKR determinant, the zeroes of which determine the energy bands, and so the bands themselves will be affected by an amount of the order of a millielectronvolt. To find the anisotropy energy these bands have to be integrated over the Brillouin zone and so the new coupling could potentially be responsible for a similar change in the calculated anisotropy energy. Therefore, not including it will mean that the uncertainties in the calculation will be greater than the quantity being calculated.

Secondly, the theory of Strange and co-authors (1989a) has proved very successful in its use for the interpretation of relativistic spectroscopies such as magnetic dichroism in x-ray absorption (Ebert *et al* 1991). Most of this theory has assumed an incident beam perpendicular to the surface of the magnetic material and parallel to the direction of the moment. This work has usually been done in the dipole approximation. Angular

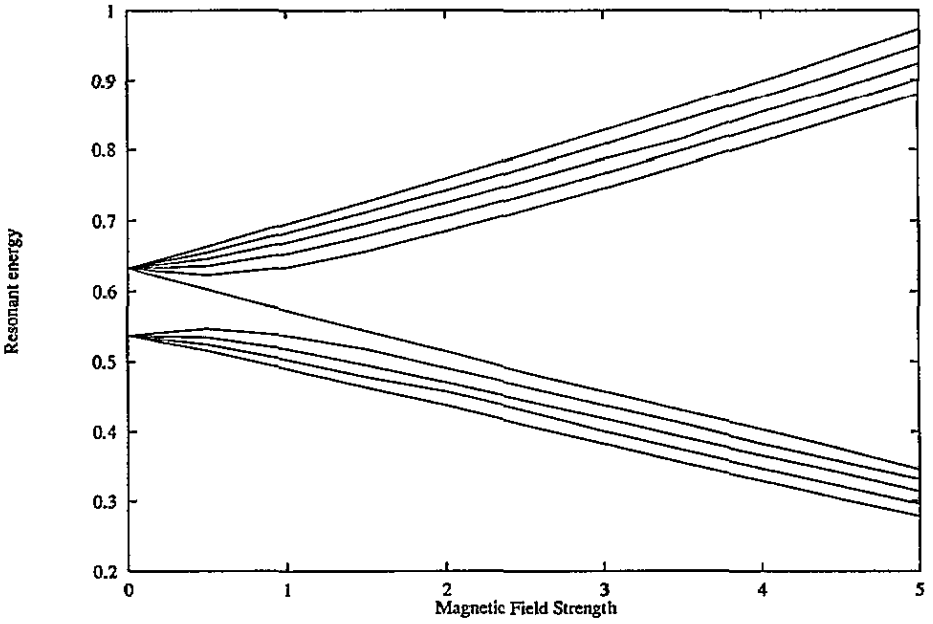

Figure 17. The Zeeman effect in the $l = 2$ levels of platinum. The lowest line has $m_j = 1.5$, the line that crosses from the upper set to the lower set has $m_j = -2.5$ and the upper line has $m_j = 2.5$. As m_j changes by one unit from one phase shift to the next, the values of m_j for all other phase shifts can be determined.

variations in the dichroism may well require the full coupling described above for a complete description. Also, going beyond the dipole approximation in such work gives us terms in the absorption rate that are several orders of magnitude smaller than the dipole absorption rate. Again, to obtain really meaningful results the extra coupling described in this paper must be included.

One can ask how significant the new coupling described here is compared with other approximations made in the calculation of observables. In particular, the solution of the Kohn–Sham-Dirac equations for transition metals using KKR methods is usually terminated at $l = 2$. Our calculations indicate that terminating the calculations here introduces an uncertainty into the results which is of the same order as that introduced by ignoring the coupling described in this paper.

This work removes one of the approximations which go into first principles descriptions of the electronic structure of magnetic materials. There are still approximations remaining in the theory however. Firstly, we have performed a Gordon decomposition of the four-current. Ideally we would like to avoid this and allow the field to couple to the orbital angular momentum of the electrons as well as to their spin. This is closely allied to the ultimate desire within density functional theory to solve equation (1) directly. Secondly we have assumed zero field outside the enscribed sphere. Formally, solutions of the Dirac equation inside the sphere should be matched to solutions of the Dirac equation with a constant potential and a constant magnetic field (Johnson and Lippman 1949). It is known that the electrons in the interstitial region can make a significant contribution to the magnetic moment. Such contributions would not be treated correctly in the multiple scattering generalization of this work. Also, we have taken our field inside the sphere to be

spherically symmetric in magnitude and of constant direction.

Acknowledgments

We would like to thank Dr J B Staunton for several useful discussions.

References

Ackermann B and Feder R 1984 *Solid State Commun.* **49** 489
Baym G 1974 *Lectures on Quantum Mechanics* (New York: Benjamin)
Daalderop G H O, Kelly P J, Schuurmans M F H and Jansen H J F 1989 *J. Physique Coll.* **49** C8 93
Ebert H, Strange P and Gyorffy B L 1988 *J. Phys. F: Met. Phys.* **18** L135
Ebert H, Wienke R, Schutz G and Temmerman W M 1991 *Physica* B **172** 71
Feder R, Rosicky F and Ackermann B 1983 *Z. Phys* B **52** 31
Gotsis H J and Strange P 1994 *J. Phys.: Condens. Matter* at press
Guo G Y, Temmerman W M and Ebert H 1992 *J. Magn. Magn. Mater.;Proc. Int. Conf. on Magnetism* (Amsterdam: North-Holland)
Gyorffy B L 1982 *The Electronic Structure of Complex Systems (NATO ASI Series B)* vol 113, ed P Phariseau and W M Temmerman
Hohenberg P and Kohn W 1964 *Phys. Rev.* B **136** 864
Johnson M H and Lippman B A 1949 *Phys. Rev.* **26** 828
Kohn W and Rostoker N 1954 *Phys. Rev.* **94** 1111
Kohn W and Sham L J 1965 *Phys. Rev.* **140** A1133
Korringa J 1947 *Physica* **13** 392
Lloyd P and Smith P V 1972 *Adv. Phys.* **21** 89
Loucks T L 1967 *The Augmented Plane Wave Method* (New York: Benjamin)
MacDonald A H, Daams J M, Vosko S H and Koelling D D 1981 *Phys. Rev.* B **23** 6377
MacDonald A H and Vosko S H 1979 *J. Phys. C: Solid State Phys.* **12** 2977
Newton R G 1966 *Scattering Theory of Waves and Particles* (New York: McGraw-Hill)
Rajagopal A K 1978 *J. Phys. C: Solid State Phys.* **11** L943
Ramana M V and Rajogopal A K 1979 *J. Phys. C: Solid State Phys.* **12** L845
Rose M E 1961 *Relativistic Electron Theory* (New York: Wiley)
Staunton J, Gyorffy B L and Weinberger P 1980 *J. Phys. F: Met. Phys.* **10** 2665
Strange P, Durham P J and Gyorffy B L 1991a *Phys. Rev. Lett.* **67** 3590
Strange P, Ebert H, Staunton J B and Gyorffy B L 1989a *J. Phys.: Condens. Matter* **1** 2959
—— 1989b *J. Phys.: Condens. Matter* **1** 3947
Strange P and Gyorffy B L 1990 *J. Phys.: Condens. Matter* **2** 9451
Strange P, Staunton J B and Ebert H 1989c *Europhys. Lett* **9** 169
Strange P, Staunton J and Gyorffy B L 1984 *J. Phys. C: Solid State Phys.* **17** 3355
Strange P, Staunton J B, Gyorffy B L and Ebert H 1991b *Physica* B **172** 51
Von Barth U and Hedin L 1972 *J. Phys. C: Solid State Phys.* **5** 1629